Journal of Hazardous Materials 414 (2021) 125553

Contents lists available at ScienceDirect

Journal of Hazardous Materials

journal homepage: www.elsevier.com/locate/jhazmat

Research Paper

Graphene environmental biodegradation: Wood degrading and saprotrophic fungi oxidize few-layer graphene

Fabio Candotto Carniel [a,*,1], Lorenzo Fortuna [b,1], Davide Zanelli [a], Marina Garrido [b], Ester Vázquez [c,d], Viviana Jehová González [d], Maurizio Prato [b,e,f], Mauro Tretiach [a]

[a] Department of Life Sciences, University of Trieste, via L. Giorgieri 10, Trieste I-34127, Italy
[b] Department of Chemical and Pharmaceutical Sciences, University of Trieste, via L. Giorgieri 1, Trieste I-34127, Italy
[c] Facultad de Ciencias y Tecnologías Químicas, Universidad de Castilla-La Mancha, Ciudad Real E-13071, Spain
[d] Instituto Regional de Investigación Científica Aplicada (IRICA), Universidad de Castilla-La Mancha, Ciudad Real E-13071, Spain
[e] Center for Cooperative Research in Biomaterials (CIC biomaGUNE), Basque Research and Technology Alliance (BRTA), Paseo de Miramón 182, Donostia San Sebastián E-20014, Spain
[f] Basque Foundation for Science, Ikerbasque, Bilbao E-48013, Spain

ARTICLE INFO

Editor: Dr. R. Debora

Keywords:
Fungal decomposers
Laccase
Lignin peroxidase
Raman analysis
2d materials

ABSTRACT

The environmental biodegradability profile of graphene related materials (GRMs) is important to know in order to predict whether these materials will accumulate in soil or will be transformed by primary decomposers. In this study, few-layer graphene (FLG) was exposed to living and devitalized axenic cultures of two white-rot basidiomycetes (*Bjerkandera adusta* and *Phanerochaete chrysosporium*) and one soil saprotrophic ascomycete (*Morchella esculenta*) with or without lignin, for a period of four months. Over this time, the increase of fungal biomass and presence of H_2O_2 and oxidizing enzymes [laccase/peroxidase and lignin peroxidase (LiP)] in growth media was assessed by gravimetric and spectrophotometric measurements, respectively. Raman spectroscopy and transmission electron microscopy (TEM) were used to compare the structure of FLG before and after incubation. All of the test fungi decreased pH in growth media and released H_2O_2 and laccase/peroxidase, but only basidiomycetes released LiP. Independent of growth media composition all fungi were found to be capable to oxidize FLG to a graphene oxide-like material, including *M. esculenta,* which released only laccase/peroxidase, i.e. the most common enzymes among primary decomposers. These findings suggest that FLG involuntarily released into terrestrial environments would likely be oxidized by soil microflora.

1. Introduction

Graphene is considered to be one of the ground-breaking materials of the future thanks to its extraordinary chemical and physical properties, making it suitable for numerous applications, including optoelectronics, automotive, medical, energy storage and mobile communications (Novoselov et al., 2012). Since its isolation in 2004 (Novoselov et al., 2004), the number of patented applications and technologies have increased exponentially over time and fruits of the research are now becoming ubiquitous in society; a few examples include sports equipment, ear pods, phone dissipators, bicycle tyres and brake pads, asphalts for road paving, and many more (for a list see www.graphene-info.com). Singularly, these objects only contain a small amount of graphene and graphene related materials (GRMs) which may inadvertently be released into the environment during the production, use or discharge processes. However, some applications involve deliberate release of GRMs for specific aims, such as pest-control (An et al., 2017; Liu et al., 2017; Miraftab and Xiao, 2019; Wang et al., 2019) or delivery of drugs and fertilizers (An et al., 2017; Kabiri et al., 2017; Andelkovic et al., 2018) in crops. Unfortunately, the environmental fate of graphene and GRMs is still largely unknown, because only chemical-physical degradative processes by abiotic means have been investigated to date (Huh et al., 2011; Radich et al., 2014).

The role of organism-mediated degradation processes on the environmental fate of these materials have largely been ignored (Fadeel et al., 2018). In terrestrial habitats, dead organic matter is progressively

* Corresponding author.
E-mail address: fcandotto@units.it (F. Candotto Carniel).
[1] These authors equally contributed in this work

https://doi.org/10.1016/j.jhazmat.2021.125553
Received 3 September 2020; Received in revised form 2 February 2021; Accepted 25 February 2021
Available online 1 March 2021
0304-3894/© 2021 The Authors. Published by Elsevier B.V. This is an open access article under the CC BY-NC-ND license (http://creativecommons.org/licenses/by-nc-nd/4.0/).

mineralized for use as an energy source into carbon and other nutrients by primary decomposers such as bacteria and fungi. Fungi have generally been described as the most efficient decomposers, because they use hyphae to penetrate the substrate, while bacteria are restricted to growing and feeding on exposed surfaces of organic matter. In addition, some fungi are known to degrade macromolecules recalcitrant to the attack of bacteria (Boonchan et al., 2000).

A specialized group of wood-degrading basidiomycetes (so-called "white rots") is capable of degrading lignin which is one of the most abundant, highly heterogeneous and recalcitrant biopolymers in nature. To break down lignin, fungal mycelia produce and release a complex exudate of a plurality of oxidative enzymes (e.g. lignin-, Mn-dependent-, versatile-peroxidases etc.), their substrates (e.g·H_2O_2, veratryl alcohol etc.) and biosurfactants (Ostrem Loss and Yu, 2018). The catalytic cycle of these enzymes generates highly oxidizing radical species, which can oxidize non-phenolic (LiP) or phenolic (MnP) compounds of lignin, thus fragmenting it (Ten Have and Teunissen, 2001). Moreover, the presence of lignin fragments appears to stimulate even further production and release of the aforementioned exudates (Rogalski et al., 1991). Biosurfactants enhance the process by decreasing surface and interfacial tension forces of degraded molecule fragments making them more hydrophilic and thus, bioavailable (Volkering et al., 1995).

This capability was exploited in the past to develop technologies for the removal of persistent pollutants from the environment but also for industrial purposes. In fact, these fungi can successfully degrade xenobiotic molecules (Pinedo-Rivilla et al., 2009). For example, some white-rot fungi (as do numerous bacteria) can degrade a variety of organic pollutants, from the less persistent polycyclic aromatic hydrocarbons (i.e. benzo-a-pyrene) (Ostrem Loss and Yu, 2018) to highly persistent organo-halogenated compounds such as PCBs, dioxins and furans (Mori and Kondo, 2002; Stella et al., 2017). White rots and other basidiomycetes were thus used for bioremediation of industrial wastewaters and contaminated soils (Robinson and Nigam, 2008; Faraco et al., 2009; Fan et al., 2013). Examples of possible industrial applications for white rots degradative process were the "bleaching" of wood pulp for the paper industry (Kondo et al., 1994) and the solubilisation of hard and low-rank coal in order to obtain water soluble low-molecular weight polymers with added value for further industrial processes (Hofrichter et al., 1997; Catcheside and Ralph, 1999). The studies on coals showed that white-rots were able to cleave and transform coal seams thanks to the mechanical action of hyphae and to the enzymes they use to degrade dead organic material, particularly LiP and MnP, respectively (Catcheside and Ralph, 1999).

For these reasons white-rots (together with other saprotrophic fungi) may be the best candidates to study the degradation of GRMs, or at least for their transformation into chemical species more vulnerable to a wide range of primary decomposers, such as less aggressive fungi and bacteria. The only few studies available on this topic tested the degradative capabilities of the white-rots and their purified lignin peroxidase (LiP) on already oxidized carbon nanomaterials (Chen et al., 2017; Yang et al., 2019). Oxidized forms of graphene, such as graphene oxide (GO) and reduced GO, possess defects on their lattice making them more prone to be oxidized by degradative extracellular enzymes, such as peroxidases (Kotchey et al., 2012). By comparison, graphene and few-layer graphene (FLG) are made of almost 100% carbon atoms organized in a regular two-dimensional honeycomb structure (Geim, 2009) and should therefore be more resistant to radicals produced by the fungal extracellular enzymes. Hence, the aim of this work was to test the capability of white-rots basidiomycetes and saprotrophic ascomycetes in the biodegradation of FLG. For this purpose, the basidiomycetes *Bjerkandera adusta* and *Phanerochaete chrysosporium*, and the ascomycete *Morchella esculenta* were selected for (*i*) well-known degradative capabilities, even towards recalcitrant xenobiotic molecules, (*ii*) production and release of different pools of degradative enzymes (Tuor et al., 1995; Gramss et al., 1999), and (*iii*) because are representative of wood- or litter degrading organisms. To test if these fungi are able to degrade FLG, they were grown for up to four months in liquid cultures enriched with FLG, which was analysed by Raman and transmission electron microscopy (TEM) at the end of the incubation period.

2. Materials and methods

2.1. FLG preparation and characterization

FLG was prepared by the ball milling treatment described by González-Domínguez and coauthors (Gonzáles-Domínguez et al., 2018) starting from a mixture of graphite (7.5 mg of SP-1 graphite powder, Bay Carbon, USA), and melamine (22.5 mg of 1,3,5-triazine-2,4,6-triamine, Sigma-Aldrich, D). The resulting solid mixture was suspended in water and melamine was washed away by dialyzing against water. The liquid fraction with stable sheets in suspension (FLG) was lyophilized and when required, the material was re-suspended in water to a final concentration of 100 μg mL^{-1}. FLG powders were characterized by thermogravimetric analysis (TGA) with a TGA Q50 (TA Instruments, USA) at 10 °C per minute under atmospheric nitrogen, from 100 °C to 800 °C. An aliquot of the FLG suspension was drop-casted onto a Si wafer, dried on a hot plate and analysed with an inVia Raman Microscope (Renishaw, UK) at 532 nm with a 100 × objective and an incident power of 1% (1 mW μm^{-2}). Quantitative analyses of C, H, N and O was carried out with a LECO CHNS-932 (LECO Corporation, USA) elemental analyser. Seven μL of the FLG suspension was cast onto nickel grids (3 mm, 200 mesh), dried under vacuum and observed with a high-resolution TEM at an accelerating voltage of 200 kV. Images were analysed with Fiji software to calculate the lateral size distribution.

2.2. Fungi cultures and growth

Axenic strains of the white-rot fungi basidiomycetes *Bjerkandera adusta* (Willd.) P. Karst. (strain nr. CBS 595.78) and *Phanerochaete chrysosporium* (Fr.) P. Karst. (CBS 246.84), and the soil ascomycete *Morchella esculenta* (L.) Pers. (CBS 172.73) were purchased from Westerdijk Fungal Biodiversity Institute (Utrecht, NL). The fungi were subcultured in Microbox Junior 40 vessels (Duchefa Biochemie, NL) filled with 20 g of solid malt extract agarose medium comprised of 30 g L^{-1} malt extract; 5 g L^{-1} peptone from meat; 15 g L^{-1} agar and grown under dim light conditions (c. 18 μmol photons m^{-2} s^{-1}) using a cycle of 14/10 hrs of light/darkness at 20 °C until the development of abundant biomass.

2.3. Fungal growth with FLG

A preliminary experiment was carried out to assess whether the presence of FLG in culture media had a negative effect on growth of the test fungal species. Fungal biomass was harvested from solid cultures (described in Section 2.2) weighed, re-suspended in liquid malt extract glucose medium (MEG) (Muzikář et al., 2011) to a concentration of 50 mg mL^{-1} (fresh weight) and homogenised with a Tissue Grinder (VWR, U.S.A.). Aliquots of 200 μL were inoculated into sterile Erlenmeyer's flasks filled with 10 mL of MEG enriched with 0, 12.5, and 50 μg mL^{-1} of FLG. Cultures were kept in the dark at 20 °C for 1 (T1), 2 (T2) and 4 (T3) months. Each culture condition for each time point (T1–3) was prepared in triplicate. Cultures were periodically refilled with pure or lignin-enriched MEG to compensate for water evaporation and nutrient depletion for the duration of the trial.

2.4. Degradation experiment

To assess the capability of test fungi to degrade FLG, 200 μL of homogenized fungal suspensions were inoculated into sterile 25 mL Erlenmayer's flasks filled with 10 mL of pure MEG (control cultures; Ctrl) and in MEG enriched with FLG, colloidal lignin or both (FLG and/or lignin-enriched cultures: respectively, F, L, F+L) to a concentration of

25 μg mL^{-1}; colloidal lignin was prepared as per Kurek et al. (1990). In order to determine whether the presence of biological materials (i.e. cell-wall and cytoplasmic components released by the dead cells) and/or growth media compounds contribute to modify FLG on their own, two additional sets of flasks containing FLG-enriched MEG were prepared: one was not inoculated (NI) and the other was inoculated (one flask per species) with dead mycelia (DM; devitalized in an autoclave). Control, FLG- and/or lignin-enriched cultures were prepared in triplicate and grown under the same conditions described in Section 2.3.

2.5. Assessment of FLG transformation/degradation by fungi

120 μL of FLG-enriched MEG was sampled at T0 (i.e. prior to inoculation) and at T3 from treated, NI and DM cultures. Sampled aliquots were treated with three-step sequential washings (1: SDS 30 g L^{-1}; 2: HCl 1 M; 3: 100% ethanol) following Yang et al. (2019) to free FLG from remaining mycelium. At each step, FLG was separated from the washing solution by vacuum-filtration over a 0.025 μm mesh MF-Millipore filter-membrane (diam. 2.5 cm, Merck, D). FLG was recovered by soaking the filter-membrane in 1 mL of Milli-Q H_2O, and then sonicating the membrane for 5 mins. Prior to the experiments, the possible effect of this washing process on FLG was tested using Raman spectroscopy. No changes in the Raman spectrum of FLG were detected. Two aliquots of 30 and 7 μL were collected and drop-casted onto Polysine glass slides (Thermo-Scientific, U.S.A.; n = 3) and Pure Carbon grids (3 mm, 200 mesh; n = 3), respectively. Glass slides and TEM grids were dried over silica gel for 48 h and then analysed as follows. Raman analysis was carried out with an inVia Raman Microscope (Renishaw, UK) focussing on between 6 and 30 FLG flakes at 532 nm with a 50 × objective and an incident power of 1% (1 mW μm^{-2}). TEM observations were made with a Philips EM208 electron microscope (Philips, N) operating at 100 kV and equipped with a Quemesa EMSIS camera (EMSIS, D).

2.6. Peroxidase/laccase and LiP activity assessment

2 mL of control (T0) and FLG enriched MEG were next filtered with a syringe filtered-tip (0.2 μm). The control sample was used to detect baseline activity of generic peroxidases/laccases and lignin peroxidases (LiP) in growth media using colorimetric methods, by providing the enzyme-specific primary substrate, i.e. 2,2-azinobis-(3-ethylbenzothiazoline-6-sulfonate) (ABTS), veratryl alcohol (VA), and H_2O_2 as appropriate. The activity of generic peroxidase/laccase was detected following the enzyme-dependent production of ABTS cationic radical ($ABTS^{\bullet+}$)(Bach et al., 2013) by adding 168 μL of ABTS (84 mM) and 0.4 μL of H_2O_2 (210 mM) [Note: the addition of H_2O_2 was only necessary for *B. adusta* and *P. chrysosporium* cultures] to 832 μL of filtered MEG. Similarly, the presence of LiP was detected by measuring the production of veratraldehyde which is a by-product of LiP activity derived by VA oxidation (Tien and Kirk, 1988). For this assay, 5.6 μL of VA (1.5 M) and 0.4 μL of H_2O_2 (210 mM) were added to 996 μL of filtered MEG. The absorbance change due to the accumulation of $ABTS^{\bullet+}$ and veratraldehyde was followed over an incubation period of 45 mins, at 734 and 310 nm respectively with a Jenway 7315 UV/VIS spectrophotometer (Bibby Scientific, UK). When the enzymatic assays provided negative results, spectrophotometric measurements were repeated after 24 hr. The absorbance values of both enzymatic assays were referred to that of blank samples prepared without the addition of H_2O_2.

2.7. pH and H_2O_2 content in growth media

At the completion of the experiment, when all fungal cultures had reached the stationary growth phase, the remaining growth medium of control and FLG- and/or lignin-enriched cultures was divided into two aliquots of ~3 and 0.5 mL. The first aliquot was used to measure pH using a Crison Basic pH-meter (Crison, S). The second aliquot was filtered (as explained previously) with a syringe filtered-tip (0.2 μm), diluted 1:1 with pure chloroform, vortexed and centrifuged for 1 min at 350 × g to remove protein and enzymes which might cause H_2O_2 depletion over time. Supernatant was then recovered and H_2O_2 content was quantified colorimetrically using the Amplex Red® kit (Life Technologies, USA). Absorbance change was monitored at 560 nm with a microplate reader BioTek ELx808 (Biotek instruments, USA). H_2O_2 concentration was evaluated using a calibration curve constructed over a 0.625–50 μM range. Quality of measurements was evaluated by the analysis of control samples with a known amount of H_2O_2.

2.8. Growth dynamic

The biomass increase of fungal cultures was gravimetrically monitored from T1-T3 during both the preliminary and degradation experiments. Bulk mycelium was separated from the remaining medium using tweezers. Very small fragments or conidia were subsequently collected after centrifuging (2 min at 9000 × g). The remaining supernatant was discarded, and biomass recovered by centrifugation was then pooled with the bulk mycelium in pre-weighed Eppendorf's tubes, soaked in liquid N_2 and freeze-dried for 72 hr. Biomass dry weights (n = 3) were measured by weighing the tubes and subtracting the tube's tare weight.

2.9. Data analysis

Biomass measurements related to the preliminary and degradation experiments were used to test whether selected FLG concentrations (0, 12.5 and 50 μg mL^{-1}) or growth media composition (Ctrl, F, L, F+L) affected fungal growth over time (T1–3). In particular, species-specific biomass average values calculated for each growth condition were statistically compared with a two-way ANOVA, selecting "time points" and the "FLG concentrations" or "time points" and "growth media composition" as categorical factors for the results of the preliminary and biodegradation experiments, respectively. Absorbance values related to the two enzymatic assays were expressed as μmol of ABTS or VA standardized per biomass unit. Significant difference in terms of H_2O_2 content in species-specific fungal cultures as a function of growth media composition (i.e. Ctrl, F, L, F+L) at T3 were assessed by non-paramatetric Kruskal-Wallis ANOVA. Before statistical analysis, Raman spectra were pre-processed in order to remove spikes and fluorescence signal due to the presence of residual fungal compounds in analysed samples. Spectra were corrected by subtracting baseline signal with polynomial functions and smoothed using the Savitzky-Golay Smoothing Filter algorithm (Lieber and Mahadevan-Jansen, 2003). Then, to verify whether fungi may have modified the FLG, the I(D)/I(G) values derived from Raman spectra of FLG-enriched cultures at stationary phase (i.e. T3) were analysed with a two-way ANOVA. This statistical comparison was carried out selecting the absence/presence of the inoculum (i.e. "inoculum") and the presence/absence of lignin or dead mycelia (i.e. "compounds") as categorical factors. A further, deeper statistical analysis of whole Raman spectra was then carried out using multivariate techniques, such as Principal Component Analysis (PCA) and Cluster Analyses (CA) with the aim to identify further differences in the spectra of FLG flakes exposed to different fungal species in diverse growth media. Differences among the groups identified by multivariate analysis were verified by one-way ANOVA using the Raman bands as the response variable, which mainly contribute to explain the variance of all collected Raman spectra (n = 248).

3. Results and discussion

In vitro fungal culturing has frequently been used to study the way in which fungi decompose dead organic matter and litter (Ten Have and Teunissen, 2001), and persistent organic pollutants (Pinedo-Rivilla et al., 2009). This approach was used here to verify if two wood-degrading white-rot basidiomycetes and one saprotrophic ascomycete are capable of biodegrading FLG. However, even under ideal and

controlled conditions, the presence of a potentially toxic substance in the growth environment could negatively affect fungal physiology, altering growth or even causing death of the organism. To date, only Yang and colleagues (Yang et al., 2019) have observed negative effects on morphological structure and mycelium development of *P. chrysosporium* when exposed to high concentrations of graphene oxide (GO $\geq$ 2 mg mL^{-1}). As yet there are no reports in the literature about toxic effects of FLG on fungi, although it is known that FLG can cause negative effects principally because of the hardness and thinness of its flakes (Montagner et al., 2017). In this study, the effect of GRMs on the growth of selected fungi was preliminary evaluated by incubating liquid fungal cultures with FLG concentrations from 0 to 50 μg mL^{-1} for one (T1), two (T2) and four (T3) months. The results show that up to 50 μg mL^{-1} of FLG, fungal growth was not significantly affected (Fig. S1; Table S1), even if hyphae were in direct contact with FLG aggregates (see Fig. S2b, d). For these reason, the experiment on fungal biodegradation capabilities was carried out using an FLG concentration (25 μg mL^{-1}) intermediate to the aforementioned range.

3.1. Fungal growth and micro-environmental changes supporting biodegradative processes

Micro-environmental changes supporting biodegradative processes were monitored over T1-T3 by assessing the presence of oxidizing enzymes (laccase/peroxidase and lignin peroxidase) and H_2O_2 in growth media of different composition, i.e. pure malt extract glucose medium (MEG; Ctrl) and MEG enriched with 25 μg mL^{-1} of FLG (F), lignin (L) or both (F + L).

At T1, when fungal cultures developed a biomass ranging from 21 ± 6 mg (dry weight, *M. esculenta*) to 26 ± 2 mg (*B. adusta*) (Fig. 1a–c), $ABTS^{\bullet+}$ production related to laccase/peroxidase activity, was 7.6 and 6.7 μM mg^{-1} (on fungal dry weight; dw) in *B. adusta* and *P. chrysosporium* growth media, respectively (Fig. 1d, e), whereas it was not detectable in *M. esculenta* (Fig. 1f), even after 24 h of incubation (see materials and methods).

As expected, activity of lignin peroxidase (LiP), expressed as a veratraldehyde content increase, was only detected in *B. adusta*

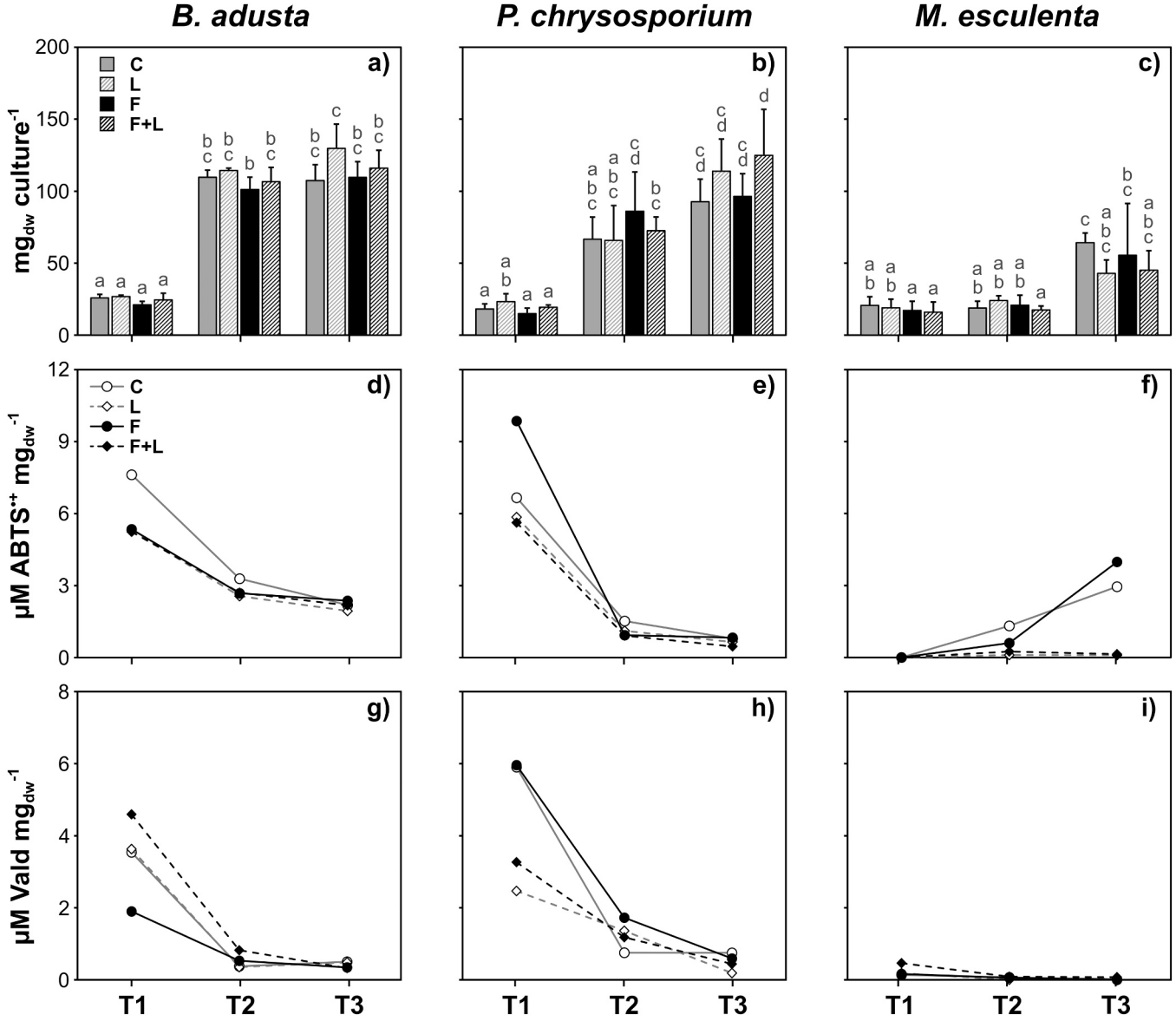

Fig. 1. Fungal biomass (a-c) in *Bjerkandera adusta*, *Phanerochaete chrysosporium* and *Morchella esculenta* cultures grew in pure growth medium (C) or enriched with 25 μg mL^{-1} of lignin (L), FLG (F) or both (F+L) for one (T1), two (T2) and four (T3) months. Letters above bars in a-c indicate statistically significant differences (Two-way ANOVA, Tuckey's HSD post-hoc test) among cultures of the same species (n = 3). Oxidative enzymes (laccase/peroxidase and lignin peroxidase) presence in the above-mentioned growth media after T1-T3, expressed as of $ABTS^{\bullet+}$ (d-f) and veratraldehyde (Vald) (g-i) content [μM per mg of fungal dry weight (dw)].

(3.5 μM mg^{-1} dw) and *P. chrysosporium* (5.9 μM mg^{-1} dw) cultures (Fig. 1g–i), since *M. esculenta* does not produce LiP (Papinutti and Lechner, 2008).

From T1 to T2, *B. adusta* and *P. chrysosporium* increased their biomass by 4.2- and 3.7-fold respectively (Fig. 1a, b). A proportional increase in enzymatic activity in the growth media of both white-rot fungi was not observed, resulting in a decrease in both the $ABTS^{\bullet+}$ and veratraldehyde content on dry fungal biomass (Fig. 1d, e, g, h). By comparison, *M. esculenta* biomass did not significantly increase with respect to T1 (Fig. 1c). However, the $ABTS^{\bullet+}$ content in growth media became detectable after 24 h of incubation, with a maximum content of 1.3 μM mg^{-1} dw (Fig. 1f).

From T2 to T3, *B. adusta* and *P. chrysosporium* cultures stopped growing (with few exceptions) and a slight decrease in the extracellular enzymatic activity was observed (Fig. 1g, h). On the contrary, the biomass in *M. esculenta* cultures increased from 1.8- to 3.4-fold, whereas the $ABTS^{\bullet+}$ content was from 2.2 to 6.6 times higher, with respect to T2, for Ctrl and F cultures, respectively. (Fig. 1c, f). Contrary to previous reports, lignin-enriched medium (L) did not stimulate white-rot fungal growth (Fig. 1a–c) or production of lignin degrading enzymes (Fig. 1d–i) but interestingly, it appeared to decrease the laccase/peroxidase activity in *M. esculenta* growth medium (Fig. 1f) in comparison to lignin-free growth media (Ctrl and F cultures). This latter result is in good accordance with the hypothesis that laccases might use liberated phenolic lignin fragments as mediators in oxidation of the remaining lignin (Ten Have and Teunissen, 2001), hence competing with ABTS.

At T3, when all cultures reached the stationary phase, H_2O_2 content and pH in the growth media were measured. As observed for biomass and enzymatic activity measurements, H_2O_2 content differed among species, but not among growth conditions (Fig. 2a–c). The highest H_2O_2 content was detected in *M. esculenta* (122 ± 3 nM mg^{-1} dw) whereas the lowest in *P. chrysosporium* (26 ± 15 nM mg^{-1} dw) (Fig. 2b, c). The high H_2O_2 content in *M. esculenta* (~4 times higher with respect to basidiomycetes cultures) explains why the ABTS assay could be carried out without adding further amounts of this primary substrate. Importantly, growth media pH decreased from ~5.5 at T0 to ~3.0 at T3, confirming that all fungi were able to release oxidative enzymes and their primary oxidizing substrate (H_2O_2) and to decrease pH to values in the optimal range for the activity of the above-mentioned enzymes (Pollegioni et al., 2015). Hence, these measurements confirmed that all of the tested fungi created conditions needed to sustain an oxidative/degradative micro-environment, without being affected by the presence of FLG.

3.2. FLG modifications induced by white-rot and saprotrophic fungi

FLG characterization. Chemical and physical characterization revealed a high degree of purity in the FLG used in this study. Elemental analysis and weight decrease (recorded by TGA, ca. 3% at 600 °C) confirmed a lack of contamination and functional groups respectively, demonstrating that FLG was comprised of >95% C (Fig. S3). The Raman spectrum was characterized by one intense peak appearing at ~1580 cm^{-1}, the G band, and two additional less intense peaks at ~1345 and ~2700 cm^{-1}, the D and 2D bands respectively (Fig. S3). The ratio between the intensity (I) of D and G bands is an indicator of the presence of defects on the graphene lattice. In this case I(D)/I(G) = 0.46 confirming a low level of defects that is usually attributed to the edges of the micrometer sheets (Torrisi et al., 2012). Furthermore, the I(2D)/I(G) = 0.43, is consistent with values (<1) reported in the literature for this material (Ferrari et al., 2006; Mogera et al., 2015). TEM observation revealed that the average lateral size of the FLG flakes was 509 ± 233 nm, but flakes lower than 100 nm were also detected (Fig. S3c–d).

Because it lacks functional groups and defects on its lattice (Denis and Iribarne, 2013), FLG is the most similar to monolayer graphene in terms of chemical reactivity amongst all GRMs. For the above mentioned reasons, FLG was deemed to be the best candidate to challenge the enzymatic abilities of wood degrading and/or saprotrophic fungi. For this purpose, Raman analysis was used to discern reduced from oxidized forms of GRMs (Kaniyoor and Ramaprabhu, 2012) even when poorly concentrated and/or slightly covered by biological matrices (i.e. fungal material or growth media compounds) which are known to increase the fluorescence signal (Lieber and Mahadevan-Jansen, 2003). TEM was used to evaluate possible structural modifications of FLG, such as holes and flake fragmentation.

Growth media contain malt and yeast extracts, i.e. a mixture of carbohydrates, proteins and vitamins. During fungal growth, culture media progressively becomes enriched with dead mycelia which are capable of adsorbing metals (Hemambika et al., 2011) and decolorizing textile dyes (Fu and Viraraghavan, 2001; Lipczynska-Kochany, 2018); these could potentially also react with FLG. Hence, FLG was also exposed to both non-inoculated culture media (NI) and devitalized (DM) cultures in order to test if growth media compounds or dead mycelia altered the FLG lattice. Raman spectra of FLG flakes sampled from NI and DM cultures at T3 had an I(D)/I(G) and a 2D band intensity very close to that observed in untreated FLG (Fig. S4), although a slight change in the 2D band shape was observed (Fig. S4). The latter could be related to charge changes (doping) in the presence of the growth medium (Guarnieri et al., 2018).

TEM observations from NI culture media revealed the formation of FLG aggregates (regularly shaped, not translucent flakes; see Fig. 3a vs. b and d-f) which is a common phenomenon generally occurring over a few days in aqueous media (Widenkvist et al., 2009; Yang et al., 2011). These results prove that the growth media (as well as the dead mycelia) did not cause any structural alteration to the FLG lattice for the duration (4 months) of the experiment. By comparison, numerous flakes recovered from FLG-enriched cultures (F and F+L) from all of the test fungi

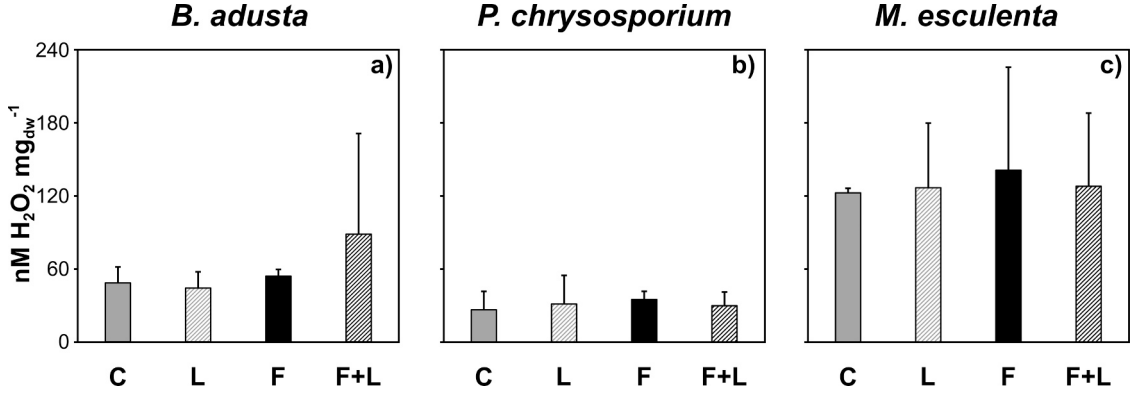

Fig. 2. H_2O_2 content in pure growth medium (C) or enriched with 25 μg mL^{-1} of lignin (L), FLG (F) or both (F+L) of *Bjerkandera adusta*, *Phanerochaete chrysosporium* and *Morchella esculenta* cultures after four months (T3) of incubation. Values are expressed as means ±s.d. (n = 3) per fungal biomass dry weight.

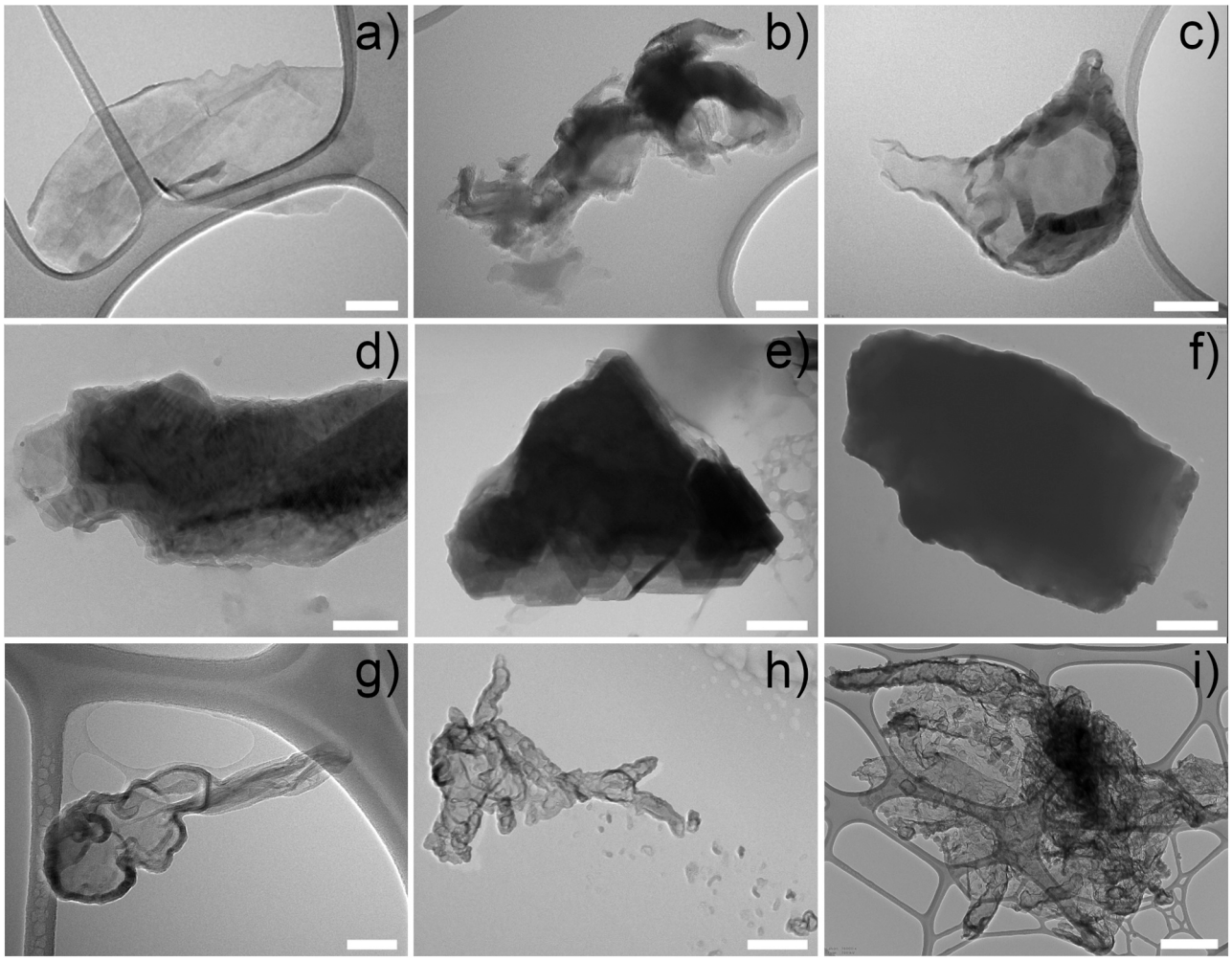

Fig. 3. TEM micrographs of representative flakes of: FLG prior to incubation with the fungi (a) and after 4 months of incubation in axenic growth medium (b); graphene oxide (Graphenea) (c); FLG after four months of incubation in devitalized (d-f) and living (g-i) cultures of *Bjerkandera adusta* (d, g), *Phanerochaete chrysosporium* (e, h) and *Morchella esculenta* (f, i). Bars: a, b, c, g = 100 nm; d, h = 200 nm; f, i = 400 nm; e = 500 nm.

had a Raman spectrum characterized by a wider and more intense D band, a shifted G band (from 1582 to 1608 cm^{-1}) and a less pronounced, or absent 2D band (Fig. S4). Hence, FLG flakes were analyzed at T3 to compare the effects of fungi once they all reached a stationary growth phase (Fig. 1a–c).

The ANOVA based comparison of the I(D)/I(G) values revealed that

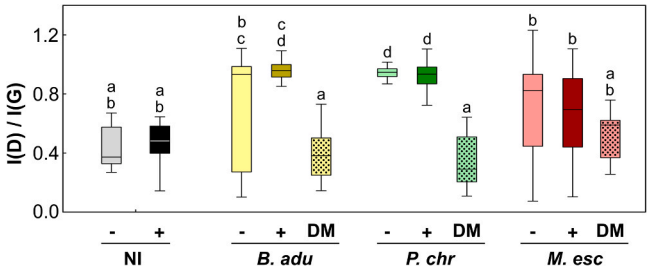

Fig. 4. Results of ANOVA-based comparison among the I(D)/I(G) values measured for FLG flakes (n = 248) recovered from non-inoculated cultures (NI) at T0 and from living (+/-) or devitalized (DM: dotted box plot) cultures of *Bjerkandera adusta* (*B. adu*), *Phanerochaete chrysosporium* (*P. chr*) and *Morchella esculenta* (*M. esc*) without (-) and with (+) lignin at T3. Boxplot middle horizontal lines represent average values, whiskers includes non-outlier range. Boxplot marked with different letters have significantly different average values.

flakes exposed to F and F+L cultures had the highest values (Fig. 4), averaging from 0.670 ± 0.270 (*M. esculenta*) to 0.938 ± 0.084 (*P. chrysosporium*). According to studies specifically aimed at evaluating graphene oxidation by Raman analysis, such D band increase clearly indicates the presence of structural imperfections created by the attachment of hydroxyl and epoxide groups on the carbon basal plane (Allen et al., 2010; Yang et al., 2009). The respective TEM observations showed that FLG flakes exposed to fungal cultures looked markedly different from those of NI and DM cultures, with the appearance of wrinkles and folding of margins (compare Fig. 3g–i with Fig. 3c).

The ANOVA outcomes confirmed that the I(D)/I(G) increase depends on interaction between “inoculum” and “compounds” (Table S2). So that, while FLG flakes from living *P. chrysosporium* cultures had significantly high I(D)/I(G) values independent of the presence of lignin (Fig. 4), those from *B. adusta* showed a significant increase of I(D)/I(G) only when the fungus was grown in lignin-enriched growth media (Fig. 4). FLG flakes from *M. esculenta* cultures by comparison had I(D)/I(G) values not significantly different from NI and the respective DM cultures, although an average increase (+40%) was observed (Fig. 4). This outcome suggests that not all of the test fungi release enzymes and molecules that are capable to significantly oxidize FLG to a GO-like material.

In order to corroborate these results, whole Raman spectra were furtherly analyzed by Principal Component Analysis (PCA) coupled with a Cluster Analysis (CA). PCA revealed that 88.2% of the variance of all

Raman spectra (n = 248) was explained by the first (76.9%) and the second (11.3%) principal components (PC; Fig. 5A): PC1 was negatively correlated with the D band intensity (r = - 0.88) and the Raman scattering recorded at 1608 cm^{-1} (r = −0.97), the D' band (Fig. 5A), whereas PC2 was positively correlated (r = 0.60) to the intensity of the 2D band. The increase of the intensity and amplitude of D and D' bands are generally associated with graphene lattice oxidation (Kaniyoor and Ramaprabhu, 2012), a process which causes shift of the G band from ~1589 cm^{-1} to ~1608 cm^{-1} (Kudin et al., 2008). Additionally, oxidized GRMs have a wider and less pronounced 2D band which is usually described as a modulated bump in this region (Kaniyoor and Ramaprabhu, 2012). Therefore, spectra projected within the first and second quarters are related to "unaltered" or non-oxidized FLG flakes (n = 105) whereas those within the third and fourth quarters are related to FLG flakes oxidized to a GO-like material (n = 143) (Fig. 5A).

Interestingly, the CA assembled the projected spectra into four groups ("a–d"; Fig. 5A), segregating unaltered flakes (group a) from oxidized flakes (groups b-d). Further, the average spectra of groups "b–d" revealed the presence of an oxidation gradient from "b" to "d", recognizable by a progressive significant increase of I(D)/I(G) and D' band intensity (Fig. S5a, b) and a decrease of the 2D band intensity (Fig. S5c). However, the groups partially overlap because they include flakes with a similar degree of oxidation.

In summary, (*i*) the ANOVA outcome (Table S2) indicating that only *B. adusta* and *P. chrysosporium* are able to induce a significant increase of I(D)/I(G) is not entirely reliable and (*ii*) FLG oxidation can be initiated by all of the fungal species independent of the enzymes they secrete (see previous section; Fig. 1). Indeed (although with different frequencies) highly oxidized FLG flakes (i.e. those classified in groups "c" and "d") were found in cultures of all three fungi (Fig. 5B): from 43% in *P. chrysosporium* to 18% in *M. esculenta*. The high percentage of unaltered FLG flakes from *M. esculenta* cultures (45%; Fig. 5B) may be explained by the relatively slow rate of growth in this species, which only reached the exponential growth phase and released a relevant quantity of oxidizing enzymes and H_2O_2 in the last two months of incubation at the tested conditions (Figs. 1, 2). Despite the slow growth (and lack of lignin peroxidase), *M. esculenta* was actually able to oxidize FLG. This result shows that laccase and peroxidase (Baldrian and Šnajdr, 2006) can promote the oxidation of chemically inert GRMs such as FLG.

3.3. Environmental relevance and further studies

In this study, it was shown that selected fungi can oxidize FLG to a GO-like material. Considering that the enzymes utilized in this study are produced by numerous primary decomposers, and that oxidative processes form the basis of organic matter biodegradation (Baldrian and Šnajdr, 2006; Sinsabaugh, 2010), it can be hypothesized that FLG involuntarily released into terrestrial ecosystems might slowly be degraded by soil microflora over extended periods, as observed for other highly recalcitrant compounds such as PAHs (Ostrem Loss and Yu, 2018) and organo-halogenated pollutants (Vyas et al., 1994; Čvančarová et al., 2012; Mori et al., 2017). Hence, it is possible that an incubation period longer than the four months tested here might have led to an advanced oxidation degree of FLG, characterized by holes onto the graphene lattice followed by flake fragmentation, as observed in in-vitro FLG degradation experiments with human myeloperoxidases (Kurapati et al., 2018). Nevertheless, it must be taken into account that, to date, nothing is known about the possible interaction with soil components of the GO-like material derived by fungal oxidation, as instead observed for other GRMs with natural organic matter in water environments (Dimiev et al., 2013; Jiang et al., 2017). Our data clearly indicate that fungal enzymes can efficiently oxidize one of the most stable GRMs, the FLG, thus weakening the hypothesis that such materials might persist in the environment for long periods. Hence, future research should address whether the fungal-derived GO-like material could be furtherly degraded until its complete conversion to CO_2 by the soil microflora.

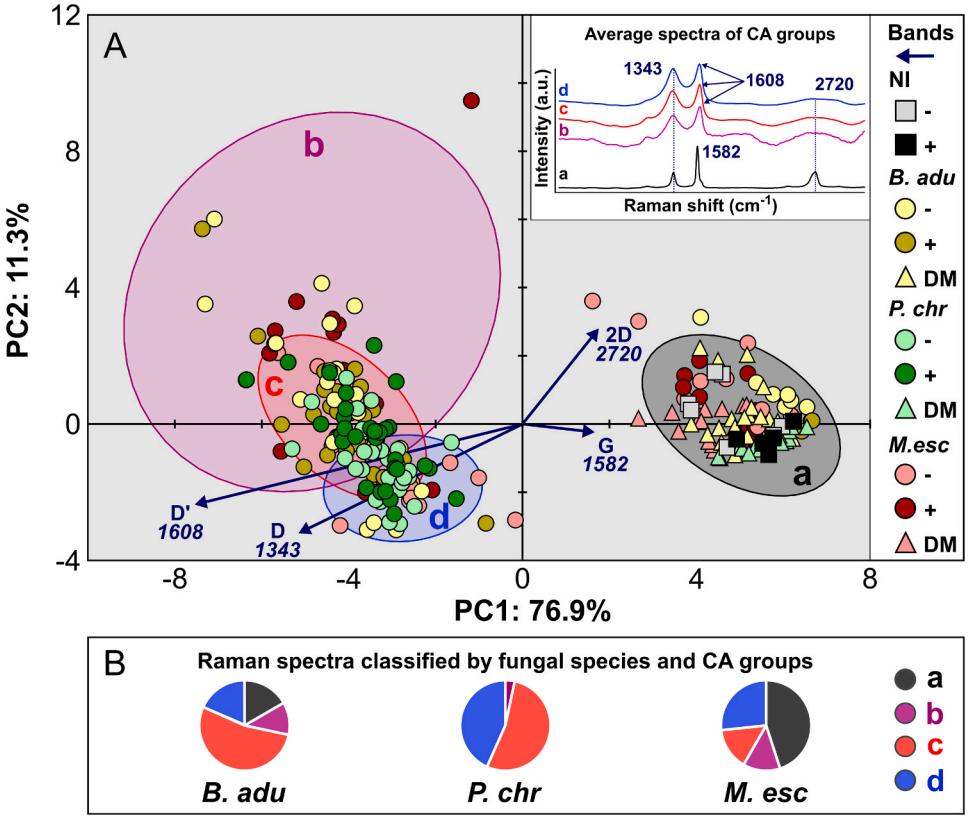

Fig. 5. Principal Component Analysis (PCA) of the Raman spectra of FLG flakes (n = 248) recovered from non-inoculated cultures at T0 (NI; squares) and from living or devitalized (DM: triangles) cultures of *Bjerkandera adusta* (*B. adu*), *Phanerochaete chrysosporium* (*P. chry*) and *Morchella esculenta* (*M. esc*) without (-; symbols in light colors) and with (+; symbols in dark colors) lignin at T3 (circles) (A). Raman spectra in the PCA space were projected according to the first two principal components (PC). Dark blue vectors represent the contribution of main Raman wavenumber shift in explaining data variance. Black, purple, red and blue concentration ellipses define four main groups (a-d, respectively) identified with Cluster Analysis (CA). The insert in (A) on the top right shows the average spectra of the four groups. Circle diagrams of the percentage of Raman spectra classified by species (living cultures) and a-d groups (B). (For interpretation of the references to colour in this figure, the reader is referred to the web version of this article.)

Funding

This work has received funding from the European Union's Horizon 2020 research and innovation programme Graphene Flagship under grant agreement No 785219 and 881603, the Spanish Ministerio de Economía y Competitividad (Project CTQ2017-88158-R) and the Junta de Comunidades de Castilla-La Mancha (Project SBPLY/17/180501/000204). M. Prato is the recipient of the AXA Chair of Bionanotechnology (2016–2023). Part of this work was performed under the Maria de Maeztu Units of Excellence Program from the Spanish State Research Agency – Grant No. MDM-2017-0720.

CRediT authorship contribution statement

Fabio Candotto Carniel: Conceptualization, Investigation, Methodology, Supervision, Visualization, Writing - original draft. **Lorenzo Fortuna**: Conceptualization, Methodology, Formal analysis, Investigation, Visualization, Writing - original draft. **Davide Zanelli**: Investigation, Methodology. **Marina Garrido**: Investigation, Formal analysis, Methodology. **Viviana Jehová González**: Investigation, Formal analysis. **Ester Vázquez:** Resources, Writing - review & editing. **Maurizio Prato**: Funding acquisition, Project administration, Resources, Supervision, Writing - review & editing. **Mauro Tretiach**: Conceptualization, Funding acquisition, Project administration, Resources, Supervision, Visualization, Writing - review & editing.

Declaration of Competing Interest

The authors declare that they have no known competing financial interests or personal relationships that could have appeared to influence the work reported in this paper.

Acknowledgements

The authors like to thank Luigi Camerlenghi (Trieste), for help in the lab, Alicia Fraile and IRICA for services in FLG characterization, Dr. Paolo Bertoncin of the TEM microscopy facility of the University of Trieste for FLG TEM observations, and Dr. Marina Tretiach (University of Sydney, AUS) for English revision.

Appendix A. Supporting information

Supplementary data associated with this article can be found in the online version at doi:10.1016/j.jhazmat.2021.125553.

References

Allen, M.J., Tung, V.C., Kaner, R.B., 2010. Honeycomb carbon: a review of graphene. Chem. Rev. 110, 132–145. https://doi.org/10.1021/cr900070d.

An, D., Liu, B., Yang, L., Wang, T.J., Kan, C., 2017. Fabrication of graphene oxide/polymer latex composite film coated on KNO3 fertilizer to extend its release duration. Chem. Eng. J. 311, 318–325. https://doi.org/10.1016/j.cej.2016.11.109.

Andelkovic, I.B., Kabiri, S., Tavakkoli, E., Kirby, J.K., McLaughlin, M.J., Losic, D., 2018. Graphene oxide-Fe(III) composite containing phosphate – a novel slow release fertilizer for improved agriculture management. J. Clean. Prod. 185, 97–104. https://doi.org/10.1016/j.jclepro.2018.03.050.

Bach, C.E., Warnock, D.D., Van Horn, D.J., Weintraub, M.N., Sinsabaugh, R.L., Allison, S. D., German, D.P., 2013. Measuring phenol oxidase and peroxidase activities with pyrogallol, l-DOPA, and ABTS: effect of assay conditions and soil type. Soil Biol. Biochem. 67, 183–191. https://doi.org/10.1016/j.soilbio.2013.08.022.

Baldrian, P., Šnajdr, J., 2006. Production of ligninolytic enzymes by litter-decomposing fungi and their ability to decolorize synthetic dyes. Enzym. Microb. Technol. 39, 1023–1029. https://doi.org/10.1016/j.enzmictec.2006.02.011.

Boonchan, S., Britz, M.L., Stanley, G.A., 2000. Degradation and mineralization of high-molecular-weight polycyclic aromatic hydrocarbons by defined fungal-bacterial cocultures. Appl. Environ. Microbiol. 66, 1007–1019. https://doi.org/10.1128/AEM.66.3.1007-1019.2000.

Catcheside, D.E.A., Ralph, J.P., 1999. Biological processing of coal. Appl. Microbiol. Biotechnol. 52, 16–24. https://doi.org/10.1007/s002530051482.

Chen, M., Qin, X., Zeng, G., 2017. Biodegradation of carbon nanotubes, graphene, and their derivatives. Trends Biotechnol. 35, 836–846. https://doi.org/10.1016/j.tibtech.2016.12.001.

Čvančarová, M., Křesinová, Z., Filipová, A., Covino, S., Cajthaml, T., 2012. Biodegradation of PCBs by ligninolytic fungi and characterization of the degradation products. Chemosphere 88, 1317–1323. https://doi.org/10.1016/j.chemosphere.2012.03.107.

Denis, P.A., Iribarne, F., 2013. Comparative study of defect reactivity in graphene. J. Phys. Chem. C 117, 19048–19055. https://doi.org/10.1021/jp4061945.

Dimiev, A.M., Alemany, L.B., Tour, J.M., 2013. Graphene oxide. Origin of acidity, its instability in water, and a new dynamic structural model. ACS Nano 7, 576–588. https://doi.org/10.1021/nn3047378.

Fadeel, B., Bussy, C., Merino, S., Vázquez, E., Flahaut, E., Mouchet, F., Evariste, L., Gauthier, L., Koivisto, A.J., Vogel, U., Martín, C., Delogu, L.G., Buerki-Thurnherr, T., Wick, P., Beloin-Saint-Pierre, D., Hischier, R., Pelin, M., Candotto Carniel, F., Tretiach, M., Cesca, F., Benfenati, F., Scaini, D., Ballerini, L., Kostarelos, K., Prato, M., Bianco, A., 2018. Safety assessment of graphene-based materials: focus on human health and the environment. ACS Nano 12, 10582–10620. https://doi.org/10.1021/acsnano.8b04758.

Fan, B., Zhao, Y., Mo, G., Ma, W., Wu, J., 2013. Co-remediation of DDT-contaminated soil using white rot fungi and laccase extract from white rot fungi. J. Soils Sediment. 13, 1232–1245. https://doi.org/10.1007/s11368-013-0705-3.

Faraco, V., Pezzella, C., Miele, A., Giardina, P., Sannia, G., 2009. Bio-remediation of colored industrial wastewaters by the white-rot fungi *Phanerochaete chrysosporium* and *Pleurotus ostreatus* and their enzymes. Biodegradation 20, 209–220. https://doi.org/10.1007/s10532-008-9214-2.

Ferrari, A.C., Meyer, J.C., Scardaci, V., Casiraghi, C., Lazzeri, M., Mauri, F., Piscanec, S., Jiang, D., Novoselov, K.S., Roth, S., Geim, A.K., 2006. Raman spectrum of graphene and graphene layers. Phys. Rev. Lett. 97, 1–4. https://doi.org/10.1103/PhysRevLett.97.187401.

Fu, Y., Viraraghavan, T., 2001. Fungal decolorization of dye wastewaters: a review. Bioresour. Technol. 79, 251–262. https://doi.org/10.1016/S0960-8524(01)00028-1.

Geim, A.K., 2009. Graphene: status and prospects. Science 324, 1530–1534. https://doi.org/10.1126/science.1158877.

Gonzáles-Domínguez, J.M., León, V., Lucío, M.I., Prato, M., Vázquez, E., 2018. Production of ready-to-use few-layer graphene in aqueous suspensions. Nat. Protoc. 13, 495–506. https://doi.org/10.1038/nprot.2017.142.

Gramss, G., Kirsche, B., Voigt, K.D., Günther, T., Fritsche, W., 1999. Conversion rates of five polycyclic aromatic hydrocarbons in liquid cultures of fifty-eight fungi and the concomitant production of oxidative enzymes. Mycol. Res. 103, 1009–1018. https://doi.org/10.1017/S0953756298008144.

Guarnieri, D., Sánchez-Moreno, P., Del Rio Castillo, A.E., Bonaccorso, F., Gatto, F., Bardi, G., Martín, C., Vázquez, E., Catelani, T., Sabella, S., Pompa, P.P., 2018. Biotransformation and biological interaction of graphene and graphene oxide during simulated oral ingestion. Small 14, 1–11. https://doi.org/10.1002/smll.201800227.

Hemambika, B., Johncy Rani, M., Rajesh Kannan, V., 2011. Biosorption of heavy metals by immobilized and dead fungal cells: a comparative assessment. J. Ecol. Nat. Environ. 3, 168–175.

Hofrichter, M., Bublitz, F., Fritsche, W., 1997. Fungal attack on coal: I. Modification of hard coal by fungi. Fuel Process. Technol. 52, 43–53. https://doi.org/10.1016/S0378-3820(97)00014-3.

Huh, S., Park, J., Kim, Y.S., Kim, K.S., Hong, B.H., Nam, J.-M., 2011. UV/Ozone-oxidized large-scale graphene platform with large chemical enhancement in surface-enhanced Raman scattering. ACS Nano 5, 9799–9806. https://doi.org/10.1021/nn204156n.

Jiang, Y., Raliya, R., Liao, P., Biswas, P., Fortner, J.D., 2017. Graphene oxides in water: assessing stability as a function of material and natural organic matter properties. Environ. Sci. Nano 4, 1484–1493. https://doi.org/10.1039/c7en00220c.

Kabiri, S., Degryse, F., Tran, D.N.H., Da Silva, R.C., McLaughlin, M.J., Losic, D., 2017. Graphene oxide: a new carrier for slow release of plant micronutrients. ACS Appl. Mater. Interfaces 9, 43325–43335. https://doi.org/10.1021/acsami.7b07890.

Kaniyoor, A., Ramaprabhu, S., 2012. A Raman spectroscopic investigation of graphite oxide derived graphene. AIP Adv. 2, 032183 https://doi.org/10.1063/1.4756995.

Kondo, R., Harazono, K., Sakai, K., 1994. Bleaching of hardwood kraft pulp with manganese peroxidase secreted from *Phanerochaete sordida* YK-624. Appl. Environ. Microbiol. 60, 4359–4436.

Kotchey, G.P., Hasan, S.A., Kapralov, A.A., Ha, S.H., Kim, K., Shvedova, A.A., Kagan, V. E., Star, A., 2012. A natural vanishing act: the enzyme-catalyzed degradation of carbon nanomaterials. Acc. Chem. Res. 45, 1770–1781. https://doi.org/10.1021/ar300106h.

Kudin, K.N., Ozbas, B., Schniepp, H.C., Prud'homme, R.K., Aksay, I.A., Car, R., 2008. Raman spectra of graphite oxide and functionalized graphene sheets. Nano Lett. 8, 36–41. https://doi.org/10.1021/nl071822y.

Kurapati, R., Mukherjee, S.P., Martín, C., Bepete, G., Vázquez, E., Pénicaud, A., Fadeel, B., Bianco, A., 2018. Degradation of single-layer and few-layer graphene by neutrophil myeloperoxidase. Angew. Chem. Int. Ed. 57, 11722–11727. https://doi.org/10.1002/anie.201806906.

Kurek, B., Monties, B., Odier, E., 1990. Dispersion of lignin in water: characterization of the phenomenon and influence on lignin enzymic degradability. Holzforschung 44, 407–414. https://doi.org/10.1515/hfsg.1990.44.6.407.

Lieber, C.A., Mahadevan-Jansen, A., 2003. Automated method for subtraction of fluorescence from biological raman spectra. Appl. Spectrosc. 57, 1363–1367. https://doi.org/10.1366/000370203322554518.

Lipczynska-Kochany, E., 2018. Humic substances, their microbial interactions and effects on biological transformations of organic pollutants in water and soil: a review. Chemosphere 202, 420–437. https://doi.org/10.1016/j.chemosphere.2018.03.104.

Liu, J., Zhao, Q., Zhang, X., 2017. Structure and slow release property of chlorpyrifos/graphene oxide-ZnAl-layered double hydroxide composite. Appl. Clay Sci. 145, 44–52. https://doi.org/10.1016/j.clay.2017.05.023.

Miraftab, R., Xiao, H., 2019. Feasibility and potential of graphene and its hybrids with cellulose as drug carriers: a commentary. J. Bioresour. Bioprod. 4, 200–201. https://doi.org/10.12162/jbb.v4i4.013.

Mogera, U., Dhanya, R., Pujar, R., Narayana, C., Kulkarni, G.U., 2015. Highly decoupled graphene multilayers: turbostraticity at its best. J. Phys. Chem. Lett. 6, 4437–4443. https://doi.org/10.1021/acs.jpclett.5b02145.

Montagner, A., Bosi, S., Tenori, E., Bidussi, M., Alshatwi, A.A., Tretiach, M., Prato, M., Syrgiannis, Z., 2017. Ecotoxicological effects of graphene-based materials. 2D Mater. 4, 1–9. https://doi.org/10.1088/2053-1583/4/1/012001.

Mori, T., Kondo, R., 2002. Oxidation of dibenzo-p-dioxin, dibenzofuran, biphenyl, and diphenyl ether by the white-rot fungus *Phlebia lindtneri*. Appl. Microbiol. Biotechnol. 60, 200–205. https://doi.org/10.1007/s00253-002-1090-9.

Mori, T., Wang, J., Tanaka, Y., Nagai, K., Kawagishi, H., Hirai, H., 2017. Bioremediation of the neonicotinoid insecticide clothianidin by the white-rot fungus *Phanerochaete sordida*. J. Hazard. Mater. 321, 586–590. https://doi.org/10.1016/j.jhazmat.2016.09.049.

Muzikář, M., Křesinová, Z., Svobodová, K., Filipová, A., Čvančarová, M., Cajthamlová, K., Cajthaml, T., 2011. Biodegradation of chlorobenzoic acids by ligninolytic fungi. J. Hazard. Mater. 196, 386–394. https://doi.org/10.1016/j.jhazmat.2011.09.041.

Novoselov, K.S., Geim, A.K., Morozov, S.V., Jiang, D., Zhang, Y., Dubonos, S.V., Grigorieva, I.V., Firsov, A.A., 2004. Electric field effect in atomically thin carbon films. Science 306, 666–669. https://doi.org/10.1126/science.1102896.

Novoselov, K.S., Fal'Ko, V.I., Colombo, L., Gellert, P.R., Schwab, M.G., Kim, K., 2012. A roadmap for graphene. Nature 490, 192–200. https://doi.org/10.1038/nature11458.

Ostrem Loss, E.M., Yu, J.H., 2018. Bioremediation and microbial metabolism of benzo(a)pyrene. Mol. Microbiol. 109, 433–444. https://doi.org/10.1111/mmi.14062.

Papinutti, L., Lechner, B., 2008. Influence of the carbon source on the growth and lignocellulolytic enzyme production by *Morchella esculenta strains*. J. Ind. Microbiol. Biotechnol. 35, 1715–1721. https://doi.org/10.1007/s10295-008-0464-0.

Pinedo-Rivilla, C., Aleu, J., Collado, I., 2009. Pollutants biodegradation by fungi. Curr. Org. Chem. 13, 1194–1214. https://doi.org/10.2174/138527209788921774.

Pollegioni, L., Tonin, F., Rosini, E., 2015. Lignin-degrading enzymes. FEBS J. 282, 1190–1213. https://doi.org/10.1111/febs.13224.

Radich, J.G., Krenselewski, A.L., Zhu, J., Kamat, P.V., 2014. Is graphene a stable platform for photocatalysis? Mineralization of reduced graphene oxide with UV-irradiated TiO_2 nanoparticles. Chem. Mater. 26, 4662–4668. https://doi.org/10.1021/cm5026552.

Robinson, T., Nigam, P.S., 2008. Remediation of textile dye waste water using a white-rot fungus *Bjerkandera adusta* through solid-state fermentation (SSF). Appl. Biochem. Biotechnol. 151, 618–628. https://doi.org/10.1007/s12010-008-8272-6.

Rogalski, J., Lundell, T.K., Leonowicz, A., Hatakka, A.I., 1991. Influence of aromatic compounds and lignin on production of ligninolytic enzymes by *Phlebia radiata*. Phytochemistry 30, 2869–2872. https://doi.org/10.1002/cber.19961290707.

Sinsabaugh, R.L., 2010. Phenol oxidase, peroxidase and organic matter dynamics of soil. Soil Biol. Biochem. 42, 391–404. https://doi.org/10.1016/j.soilbio.2009.10.014.

Stella, T., Covino, S., Čvančarová, M., Filipová, A., Petruccioli, M., D'Annibale, A., Cajthaml, T., 2017. Bioremediation of long-term PCB-contaminated soil by white-rot fungi. J. Hazard. Mater. 324, 701–710. https://doi.org/10.1016/j.jhazmat.2016.11.044.

Ten Have, R., Teunissen, P.J.M., 2001. Oxidative mechanisms involved in lignin degradation by white-rot fungi. Chem. Rev. 101, 3397–3413. https://doi.org/10.1021/cr000115l.

Tien, M., Kirk, T.K., 1988. Lignin peroxidase of *Phanerochaete chrysosporium*. Methods Enzymol. 238–249. https://doi.org/10.1016/0076-6879(88)61025-1.

Torrisi, F., Hasan, T., Wu, W., Sun, Z., Lombardo, A., Kulmala, T.S., Hsieh, G.-W., Jung, S., Bonaccorso, F., Paul, P.J., Chu, D., Ferrari, A.C., 2012. Inkjet-printed graphene electronics. ACS Nano 6, 2992–3006. https://doi.org/10.1021/nn2044609.

Tuor, U., Winterhalter, K., Fiechter, A., 1995. Enzymes of white-rot fungi involved in lignin degradation and ecological determinants for wood decay. J. Biotechnol. 41, 1–17. https://doi.org/10.1016/0168-1656(95)00042-O.

Volkering, F., Breure, A.M., Van Andel, J.G., Rulkens, W.H., 1995. Influence of nonionic surfactants on bioavailability and biodegradation of polycyclic aromatic hydrocarbons. Appl. Environ. Microbiol. 61, 1699–1705. https://doi.org/10.1128/aem.61.5.1699-1705.1995.

Vyas, B.R.M., Šašek, V., Matucha, M., Bubner, M., 1994. Degradation of 3,3′,4,4′-tetrachlorobiphenyl by selected white rot fungi. Chemosphere 28, 1127–1134. https://doi.org/10.1016/0045-6535(94)90331-X.

Wang, X., Xie, H., Wang, Z., He, K., 2019. Graphene oxide as a pesticide delivery vector for enhancing acaricidal activity against spider mites. Colloids Surf. B Biointerfaces 173, 632–638. https://doi.org/10.1016/j.colsurfb.2018.10.010.

Widenkvist, E., Boukhvalov, D.W., Rubino, S., Akhtar, S., Lu, J., Quinlan, R.A., Katsnelson, M.I., Leifer, K., Grennberg, H., Jansson, U., 2009. Mild sonochemical exfoliation of bromine-intercalated graphite: a new route towards graphene. J. Phys. D Appl. Phys. 42, 112003 https://doi.org/10.1088/0022-3727/42/11/112003.

Yang, D., Velamakanni, A., Bozoklu, G., Park, S., Stoller, M., Piner, R.D., Stankovich, S., Jung, I., Field, D.A., Ventrice, C.A., Ruoff, R.S., 2009. Chemical analysis of graphene oxide films after heat and chemical treatments by X-ray photoelectron and Micro-Raman spectroscopy. Carbon 47, 145–152. https://doi.org/10.1016/j.carbon.2008.09.045.

Yang, H., Wu, X., Ma, Q., Yilihamu, A., Yang, S., Zhang, Q., Feng, S., Yang, S.-T., 2019. Fungal transformation of graphene by white rot fungus. Chemosphere 216, 9–18. https://doi.org/10.1016/j.chemosphere.2018.10.115.

Yang, W., Widenkvist, E., Jansson, U., Grennberg, H., 2011. Stirring-induced aggregation of graphene in suspension. New J. Chem. 35, 780. https://doi.org/10.1039/c0nj00968g.